



## $\beta$ -Cell Knockout of SENP1 Reduces Responses to Incretins and Worsens Oral Glucose Tolerance in High-Fat Diet–Fed Mice

Haopeng Lin,<sup>1,2</sup> Nancy Smith,<sup>1,2</sup> Aliya F. Spigelman,<sup>1,2</sup> Kunimasa Suzuki,<sup>1,2</sup> Mourad Ferdaoussi,<sup>3</sup> Tamadher A. Alghamdi,<sup>1,2</sup> Sophie L. Lewandowski,<sup>4</sup> Yaxing Jin,<sup>1</sup> Austin Bautista,<sup>1,2</sup> Ying Wayne Wang,<sup>2,5</sup> Jocelyn E. Manning Fox,<sup>1,2</sup> Matthew J. Merrins,<sup>4</sup> Jean Buteau,<sup>2,5</sup> and Patrick E. MacDonald<sup>1,2</sup>

*Diabetes* 2021;70:2626–2638 | <https://doi.org/10.2337/db20-1235>

**SUMOylation reduces oxidative stress and preserves islet mass at the expense of robust insulin secretion. To investigate a role for the deSUMOylating enzyme sentrin-specific protease 1 (SENP1) following metabolic stress, we put pancreas/gut-specific SENP1 knockout (pSENP1-KO) mice on a high-fat diet (HFD). Male pSENP1-KO mice were more glucose intolerant following HFD than littermate controls but only in response to oral glucose. A similar phenotype was observed in females. Plasma glucose-dependent insulinotropic polypeptide (GIP) and glucagon-like peptide 1 (GLP-1) responses were identical in pSENP1-KO and wild-type littermates, including the HFD-induced upregulation of GIP responses. Islet mass was not different, but insulin secretion and  $\beta$ -cell exocytotic responses to the GLP-1 receptor agonist exendin-4 (Ex4) and GIP were impaired in islets lacking SENP1. Glucagon secretion from pSENP1-KO islets was also reduced, so we generated  $\beta$ -cell-specific SENP1 KO mice. These phenocopied the pSENP1-KO mice with selective impairment in oral glucose tolerance following HFD, preserved islet mass expansion, and impaired  $\beta$ -cell exocytosis and insulin secretion to Ex4 and GIP without changes in cAMP or  $Ca^{2+}$  levels. Thus,  $\beta$ -cell SENP1 limits oral glucose intolerance following HFD by ensuring robust insulin secretion at a point downstream of incretin signaling.**

Glucose metabolism is the primary driver for insulin secretion, stimulating electrical activity and  $Ca^{2+}$  entry to trigger the exocytosis of insulin granules. Multiple additional factors

serve to either maintain or augment the pool of secretory granules available to respond to the  $Ca^{2+}$  increase (1). These pathways could be required for robust insulin secretory responses to receptor-mediated secretagogues, such as the incretin hormones glucose-dependent insulinotropic polypeptide (GIP) and glucagon-like peptide 1 (GLP-1) (2). The action of the incretins to facilitate insulin secretion is impaired in type 2 diabetes (T2D), although the underlying mechanism appears complex (3) and could involve altered receptor signaling (4). Incretin-induced insulin secretion from human islets correlates with the ability of glucose to augment depolarization-induced insulin exocytosis in single  $\beta$ -cells (5). In mice with impaired metabolism-insulin granule coupling, achieved by  $\beta$ -cell-specific deletion of the sentrin-specific protease 1 (SENP1), we showed that the  $\beta$ -cell response to the GLP-1 receptor agonist exendin-4 (Ex4) was impaired and that the ability of dipeptidyl peptidase 4 inhibition to improve oral glucose tolerance was greatly reduced (5).

Glucose metabolism drives the export mitochondrial reducing equivalents, and the resulting redox signal relay increases the small ubiquitin-like modifier (SUMO) protease activity of SENP1 (6). A resulting deSUMOylation of exocytotic proteins, such as synaptotagmin VII, facilitates  $Ca^{2+}$ -dependent insulin granule exocytosis (7–11). This redox-dependent pathway appears impaired in T2D, likely as a result of upstream mitochondrial dysfunction, and loss of islet SENP1 results in moderate oral glucose

<sup>1</sup>Department of Pharmacology, University of Alberta, Edmonton, Alberta, Canada

<sup>2</sup>Alberta Diabetes Institute, University of Alberta, Edmonton, Alberta, Canada

<sup>3</sup>Department of Pediatrics, University of Alberta, Edmonton, Alberta, Canada

<sup>4</sup>Department of Medicine, Division of Endocrinology, Diabetes, and Metabolism, University of Wisconsin–Madison, Madison, WI

<sup>5</sup>Department of Agricultural, Food and Nutritional Science, University of Alberta, Edmonton, Alberta, Canada

Corresponding author: Patrick E. MacDonald, [pmacdonald@ualberta.ca](mailto:pmacdonald@ualberta.ca)

Received 9 December 2020 and accepted 19 August 2021

This article contains supplementary material online at <https://doi.org/10.2337/figshare.16435176>.

© 2021 by the American Diabetes Association. Readers may use this article as long as the work is properly cited, the use is educational and not for profit, and the work is not altered. More information is available at <https://www.diabetesjournals.org/content/license>.

intolerance with impaired insulin secretion (7). Somewhat contradicting this, overexpression of SENP1 induces apoptosis in  $\beta$ -cells (12), and mice lacking the SUMO-conjugating enzyme Ubc9 develop diabetes as a result of  $\beta$ -cell death (13). Effectively, SUMOylation appears required for  $\beta$ -cell viability at the cost of  $\beta$ -cell function (14). It remains unknown whether the deSUMOylating enzyme SENP1 is required for the facilitation of insulin secretory responses and glucose tolerance under metabolic stress, such as high-fat diet (HFD), or conversely, whether loss of SENP1 would protect against glucose intolerance by preserving  $\beta$ -cell mass and insulin secretion.

Here, we investigated two interrelated questions in both pancreas/gut-specific SENP1 knockout (pSENP1-KO) and  $\beta$ -cell-specific SENP1 KO ( $\beta$ SENP1-KO) mice. We asked whether the loss of  $\beta$ -cell SENP1 sensitizes mice to HFD-induced glucose intolerance and whether altered incretin responsiveness contributes to this. We find that following HFD, both pSENP1-KO mice and  $\beta$ SENP1-KO mice show a worsening of oral glucose intolerance. This is accompanied by a decreased insulin secretory response to glucose and incretin receptor activation without any difference in  $\beta$ -cell mass and little or no effect on cAMP or  $\text{Ca}^{2+}$  responses to incretin receptor activation. Our findings support a model whereby SENP1 is required to ensure the availability of releasable insulin granules. This is important for limiting oral glucose intolerance following HFD where incretins, notably plasma GIP, are increased and require a robust pool of release-competent insulin granules on which to act.

## RESEARCH DESIGN AND METHODS

### Animals, Diets, and In Vivo Studies

Pdx1-Cre mice [B6.FVB-Tg (Pdx1-cre)<sup>6</sup> Tuv/J, 014647; The Jackson Laboratories] on a C57BL/6 background and Ins1-Cre mice on a mixed C57BL/6 and SV129 background (15) were crossed with *Senp1*-floxed mice on a C57BL/6 background (7) to generate Pdx1-Cre<sup>+</sup>; *Senp1*<sup>fl/fl</sup> KO (pSENP1-KO) and Ins1-Cre<sup>+</sup>; *Senp1*<sup>fl/fl</sup> KO ( $\beta$ SENP1-KO) mice (5,7). Pdx1-Cre<sup>+</sup>; *Senp1*<sup>+/fl</sup> and Ins1-Cre<sup>+</sup>; *Senp1*<sup>+/fl</sup> mice were used as heterozygotes (pSENP1-HET and  $\beta$ SENP1-HET, respectively). Pdx1-Cre<sup>+</sup>; *Senp1*<sup>+/+</sup> and Ins1-Cre<sup>+</sup>; *Senp1*<sup>+/+</sup> mice were used as wild-type (WT) littermate controls (pSENP1-WT and  $\beta$ SENP1-WT, respectively). Genotypes were confirmed from ear notches (7). Loss of expression was confirmed by nested PCR and Western blot. At 12 weeks of age, mice were fed an HFD (60% fat, CA89067-471; Bio-Serv) for 8–10 weeks.

Mice were fasted 4–5 h prior to oral glucose tolerance test (OGTT) (16), intraperitoneal (IP) glucose tolerance test (IPGTT) (17), or insulin tolerance test (ITT) (18). OGTT and IPGTT were with dextrose at doses indicated in the figures, and ITT was with IP injection of 1 units/kg Humulin R (Eli Lilly). The timelines of OGTT, IPGTT, and ITT are shown in the figures. Tail blood was collected for glucose and insulin measurement (7). To measure total plasma GLP-1, GIP, and glucagon, before or after oral

glucose gavage (2 g/kg dextrose), tail blood was collected at the indicated times, and plasma was frozen until assay (Multi Species GLP-1 Total ELISA Kit [Millipore], Mouse GIP ELISA Kit [Crystal Chem], U-Plex Mouse Glucagon ELISA Kit [MesoScale Discovery]).

### Western Blotting

SENP1 antibody-C12 (1:500, sc-271360; Santa Cruz Biotechnology), SUMO1 antibody (1:1,000, ab133352; Abcam), and  $\beta$ -actin antibody (1:2,000, sc-47778; Santa Cruz Biotechnology) were used as primary antibodies. Anti-mouse (1:5,000, NA934V; GE Healthcare) or anti-rabbit (1:5,000, NA931V; GE Healthcare) were used as secondary antibodies. Mouse islets, gut, and brain were homogenized with 7 mol/L guanidine HCl. The protein was precipitated by addition of methanol, chloroform, and water in a 4:1:3 (v/v) ratio, and the pellet was recovered (10,000 rpm for 10 min) and dissolved in 1% SDS, 0.2 mol/L Tris, 10 mmol/L dithiothreitol, pH 6.5. Protein concentration was estimated by absorbance at 280 nm. Fifty, 10, and 10  $\mu$ g protein from islets, intestine, and brain, respectively, were separated by SDS-PAGE (7.5% gel), transferred to polyvinylidene fluoride membrane, and probed with primary antibody in the presence of 5% skim milk. For SUMOylation (19), islets were incubated in Krebs-Ringer bicarbonate HEPES buffer with 2.8 mmol/L glucose for 2 h followed by 16.7 mmol/L glucose for 15 min. Islets were washed with cold PBS and put in lysis buffer with 10 mmol/L N-ethylmaleimide (128-53-0; MilliporeSigma), 100  $\mu$ L PhosStop (1 tablet in 1 mL lysis buffer; MilliporeSigma), and 10  $\mu$ L protease inhibitor (P8340; MilliporeSigma). Ten micrograms of protein were loaded for SDS-PAGE (10% gel).

### Nested Quantitative PCR of SENP1

To evaluate KO efficiency, the cDNA encoding exons 14 and 15 was quantified by nested quantitative PCR (qPCR). Total RNA was extracted from kidney, brain, stomach, intestine, and islets using TRIzol reagent (15596018; Thermo Fisher Scientific). cDNA was prepared from total RNA (50–100 ng) with All-In-One 5X RT Master Mix (G486; Applied Biological Materials Inc.). The cDNAs of *Senp1* and *Ppia* were amplified using preamplification primers and Platinum Taq DNA polymerase (10966-018; Thermo Fisher Scientific) with the following cycling parameters: 15 cycles of 94°C for 30 s, 60°C for 10 s, 55°C for 10 s, and 72°C for 25 s. To remove Taq DNA polymerase and the primers, the PCR fragment was incubated with 4 mol/L guanidine HCl for 10 min at room temperature and precipitated with 80% ethanol in the presence of glycogen (50 mg/mL). The nested qPCR was carried out with the qPCR primers Fast SYBR Green Master Mix (438512; Applied Biosystems), 7900HT Fast Real-Time PCR System (Applied Biosystems), and the preamplified cDNAs as the templates with the following cycling parameters: 40 cycles of 95°C for 5 s and 60°C for 20 s. All primers are listed in Supplementary Table 1.

### Pancreatic Islet Isolation, Insulin, and Glucagon Secretion

Islets were isolated by collagenase digestion of the pancreas (20) and cultured overnight. Insulin secretion was measured by perfusion (7). Briefly, 25 (insulin) or 75–85 (glucagon) islets were preperfused for 30 min at 2.8 mmol/L glucose before sample collection and treated with 16.7 mmol/L glucose, Ex4 (10 nmol/L; MilliporeSigma), GIP (100 nmol/L; AnaSpec), alanine (10 mmol/L; MilliporeSigma), oleate (0.5 mmol/L, MilliporeSigma) (21,22), or KCl (30 mmol/L). Samples were collected every 1–5 min at a flow rate of 100  $\mu$ L/min, and then islets were lysed in acid/ethanol. All samples were stored at  $-20^{\circ}\text{C}$  until assayed for insulin (STELLUX Chemi Rodent Insulin ELISA; ALPCO) and glucagon (Rodent Glucagon Assay or U-PLEX Mouse Glucagon Assay; Mesoscale Discovery). For the glutamine- and leucine-stimulated insulin secretion (10 mmol/L each; MilliporeSigma), static insulin secretion was performed (23).

### Patch Clamp Analysis

Islets were handpicked and incubated with  $\text{Ca}^{2+}$ -free buffer at  $37^{\circ}\text{C}$  for 10 min before being shaken and dispersed into single cells (9). Cells were incubated in 35-mm dishes (430165; Thermo Fisher Scientific) in RPMI medium (11875; Thermo Fisher Scientific) with 11.1 mmol/L glucose, 10% FBS, and 100 units/mL penicillin/streptomycin for up to 2 days. In the experiments examining low (2.8 mmol/L) or high (10 mmol/L) glucose (Figs. 1B and C and 6A, B, J, and K), cells were preincubated in DMEM (11966025; Gibco) with 10% FBS, 100 units/mL penicillin/streptomycin, and 2.8 mmol/L glucose for 1 h prior to switching to bath solution. For the remaining experiments (5 mmol/L glucose), cells were switched to the bath without preincubation. Bath solution contained 118 mmol/L NaCl, 5.6 mmol/L KCl, 20 mmol/L tetraethylammonium, 1.2 mmol/L  $\text{MgCl}_2 \cdot 6\text{H}_2\text{O}$ , 2.6 mmol/L  $\text{CaCl}_2$ , and 5 mmol/L HEPES with glucose, Ex4 (10 nmol/L; MilliporeSigma), and/or GIP (100 nmol/L; AnaSpec) as indicated (pH 7.4 adjusted with NaOH) at  $32$ – $35^{\circ}\text{C}$ . The pipette solution contained 125 mmol/L Cs-glutamate, 10 mmol/L NaCl, 10 mmol/L CsCl, 1 mmol/L  $\text{MgCl}_2 \cdot 6\text{H}_2\text{O}$ , 0.05 mmol/L EGTA, 5 mmol/L HEPES, and 3 mmol/L MgATP (solution pH 7.15 adjusted with CsOH) with or without 0.1 mmol/L cAMP as indicated in the figure legends. Patch clamp was performed in the standard whole-cell configuration with sine+DC (direct current) LockIn function of an EPC 10 amplifier (HEKA Elektronik) 5–30 min after switching cells to the bath solution. As such, cells were preexposed to bath glucose, Ex4, or GIP prior to establishment of the whole-cell configuration. Exocytotic responses and inward  $\text{Ca}^{2+}$  currents were measured 1–2 min after obtaining the whole-cell configuration in response to 10 500-ms depolarizations to 0 mV from a holding potential of  $-70$  mV. Changes in capacitance and integrated  $\text{Ca}^{2+}$  charge entry were normalized to cell size (fF/pF and pC/pF, respectively). Mouse  $\beta$ -cells

were identified by cell size ( $>4$  pF) and half-maximal inactivation of  $\text{Na}^{+}$  currents near  $-90$  mV (24).

### $\beta$ -Cell cAMP and Intracellular $\text{Ca}^{2+}$ Imaging

The cAMP biosensor (Epac-S<sup>H187</sup>,  $K_d = 4$   $\mu\text{mol/L}$ ) (25) under control of the rat insulin promoter was expressed by adenoviral expression (26). Islets were infected immediately postisolation with 1.5  $\mu\text{L}$  of high-titer adenovirus for 2 h at  $37^{\circ}\text{C}$  and then moved to fresh media overnight. Islets from  $\beta\text{SENP1-WT}$  and  $-KO$  mice were imaged simultaneously; one group was prelabeled with 1  $\mu\text{g/mL}$  DiR (1,1-dioctadecyl-3,3,3,3-tetramethylindotricarbocyanine iodide) (Molecular Probes, Eugene, OR) for 10 min. DiR labeling had no effect on islet metabolic or  $\text{Ca}^{2+}$  oscillations (data not shown). For measurements of cytosolic  $\text{Ca}^{2+}$ , islets were preincubated in 2.5  $\mu\text{mol/L}$  FuraRed (F3020; Molecular Probes) at  $37^{\circ}\text{C}$  for 45 min before they were placed in a glass-bottomed imaging chamber (Warner Instruments) and mounted on an ECLIPSE Ti inverted microscope with a  $10\times/0.50$  numerical aperture SuperFluor objective (Nikon Instruments). The chamber was perfused with external solution containing 135 mmol/L NaCl, 4.8 mmol/L KCl, 2.5 mmol/L  $\text{CaCl}_2$ , 1.2 mmol/L  $\text{MgCl}_2$ , and 20 mmol/L HEPES (pH 7.35). The flow rate and temperature were maintained at 0.25 mL/min and  $33^{\circ}\text{C}$  using feedback control (MFCS-EZ; Fluigent). Excitation was by a SOLA SEII 365 (Lumencor) at 10% output. Single DiR images used a Chroma Cy7 cube ( $710/75\times$ , T760lpxr, 810/90 m). For FuraRed, excitation ( $430/24\times$  and  $500/20\times$ , ET type; Chroma Technology Corporation) and emission (650/60 m) filters (BrightLine; Semrock) were used with an FF444/521/608-Di01 dichroic mirror (Semrock) and reported as an excitation ratio (R430/500). The same dichroic mirror was used for cAMP biosensor fluorescence resonance energy transfer imaging, with cyan fluorescent protein excitation provided by an ET430/24 $\times$  filter and emission filters for cyan fluorescent protein and Venus emission (ET470/24m and ET535/30m; Chroma Technology) reported as an emission ratio (R470/535). Fluorescence emission was collected with an ORCA-Flash4.0 V2 Digital CMOS camera (Hamamatsu) every 6 s. A single region of interest was used to quantify the average response of each islet using Nikon Elements and custom MATLAB software (MathWorks).

### Histological Analysis

Pancreata were weighed prior to being fixed in Z-fix (VWR International) and embedded in paraffin. Blocks were sectioned at 5- $\mu\text{m}$  thickness with a total of three to five slides (each separated by 500  $\mu\text{m}$ ) for immunostaining and imaging (7). Paraffin sections were rehydrated, permeabilized, blocked, and incubated with guinea pig polyclonal insulin antibody (1:60, A0564; Dako) and mouse polyclonal glucagon antibody (1:1,000; MilliporeSigma) overnight. Sections were washed and incubated

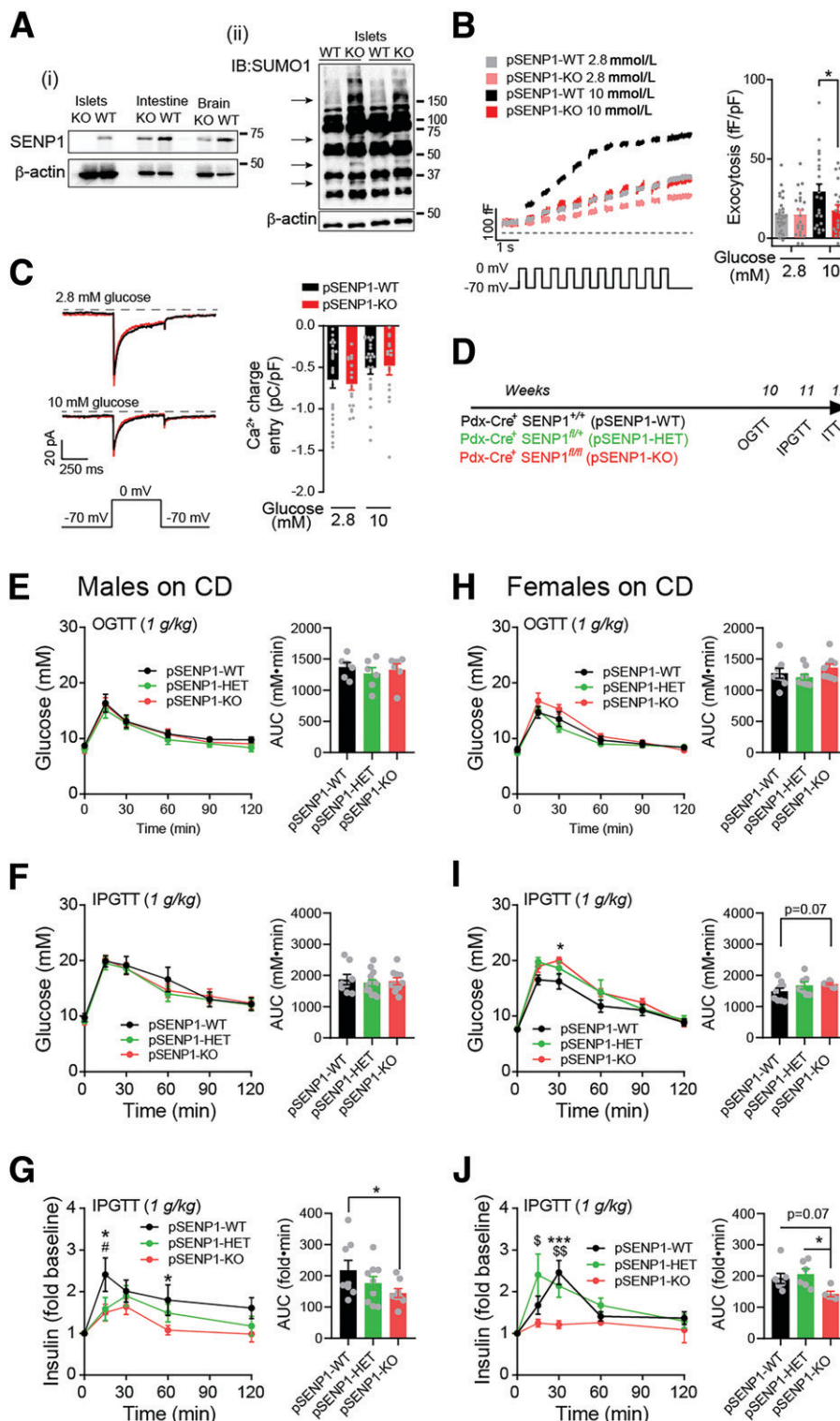


**Figure 1**—Normal glucose tolerance, but impaired insulin responses, of pSEN1-KO mice on CD. *A*: *i*) Western blot of SENP1 expression in tissues from pSEN1-WT and -KO mice. *ii*) SUMOylation profiles of islet lysates from pSEN1-WT and -KO mice showing numerous SUMOylated proteins. *B*: Representative traces (left) and average total responses of  $\beta$ -cell exocytosis elicited by a series of 500-ms membrane depolarizations from  $-70$  to  $0$  mV at  $2.8$  and  $10$  mmol/L glucose ( $n = 28, 22, 22,$  and  $20$  cells;  $n$  values correspond to graph bars from left to right, respectively). The pipette solution included  $0.1$  mmol/L cAMP. *C*: Representative traces, and average  $\beta$ -cell voltage-dependent  $Ca^{2+}$  currents elicited by a single 500-ms membrane depolarization from  $-70$  to  $0$  mV at  $2.8$  and  $10$  mmol/L glucose ( $n = 26, 18, 25,$  and  $16$  cells). The pipette solution included  $0.1$  mmol/L cAMP. *D*: Schematic diagram of experiments on CD-fed mice. *E*: OGTT in male pSEN1-WT, -HET, and -KO mice ( $n = 6, 6,$  and  $6$  mice). *F* and *G*: IPGTT in male pSEN1-WT, -HET, and -KO mice ( $n = 8, 13,$  and  $10$  mice) (*F*) and associated plasma insulin responses ( $n = 8, 9,$  and  $8$  mice) (*G*). *H*: OGTT in female pSEN1-WT, -HET, and -KO mice ( $n = 8, 9,$  and  $9$  mice). *I* and *J*: IPGTT in female pSEN1-WT, -HET, and -KO mice ( $n = 9, 7,$  and  $7$  mice) (*I*) and associated plasma insulin

with Alexa Fluor 488 goat anti-guinea pig IgG (1:500, A11073; Thermo Fisher Scientific) and Alexa Fluor 594 goat anti-mouse IgG (1:500 A11037; Thermo Fisher Scientific) for 1 h, washed, and mounted in ProLong Gold Antifade Mountant with DAPI (Life Technologies). To determine islet area, insulin-positive cells were identified with software tools from ImageJ (National Institutes of Health) and normalized to total pancreas area. The islet mass was calculated as pancreas weight  $\times$  relative islet area (as a proportion of pancreas section area). Islet size was determined by manual outlining in a blinded fashion using ZEN Pro (Zeiss) and ImageJ software.

### Statistical Analysis

GraphPad Prism 8 for Mac OS X software was used for one-way or two-way ANOVA followed by Bonferroni posttest to compare means between groups. Unbiased robust regression followed by outlier identification analysis was used for outlier identification and removal.

### Data and Resource Availability

All data generated or analyzed during this study are included in the published article and its online supplementary files. Resources generated in the current study are available from the corresponding author upon reasonable request.

## RESULTS

### Mice Lacking Islet SENP1 Develop Worsened Oral Glucose Intolerance After HFD

We previously showed that SENP1 is required for insulin exocytosis and that male pSENP1-KO mice are mildly intolerant of oral glucose (7). Because of loss of Cre expression in the previous colony, we made the pSENP1-KO mice by crossing Pdx1-Cre<sup>+</sup> mice from The Jackson Laboratories [B6.FVB-Tg (Pdx1-cre)6 Tuv/J] and Pdx1-Cre<sup>-</sup> Senp1<sup>fl/fl</sup> and confirmed loss of SENP1 (Fig. 1Ai) and increased SUMOylation (Fig. 1Aii, arrows) in islets.  $\beta$ -Cells from pSENP1-KO mice had impaired glucose-dependent facilitation of exocytosis (Fig. 1B) and unaffected voltage-dependent Ca<sup>2+</sup> currents (Fig. 1C). The pSENP1-KO mice had modest fasting hyperinsulinemia compared with littermates (Supplementary Fig. 1). We performed OGTT, IPGTT, and ITT on male and female mice at 10–12 weeks of age (Fig. 1D). Male pSENP1-KO mice were not obviously intolerant to oral or IP glucose (Fig. 1E and F and Supplementary Fig. 1A–D), despite reduced glucose-stimulated plasma insulin (Fig. 1G). Female mice exhibited a similar phenotype, with some indication of IP glucose intolerance (Fig. 1H–J and Supplementary Fig. 1E–H).

After HFD (Fig. 2A), there was no difference in insulin tolerance or fasting insulin (Fig. 2B and C), but male pSENP1-KO mice exhibited elevated fasting glucose and body weight (Fig. 2D and E). IP glucose intolerance was only modestly worsened in the pSENP1-KO mice (Fig. 2F), but these mice were clearly more intolerant of an oral glucose challenge with a decreased plasma insulin response compared with littermate controls (Fig. 2G and H). With a higher dose of glucose, there was still no worsened IP glucose intolerance in the pSENP1-KO mice (Fig. 2I), but a larger oral glucose challenge resulted in severely impaired glucose tolerance and plasma insulin (Fig. 2J and K). Similar to other reports (27), female mice were relatively resistant to HFD, and we did not observe any worsening of oral glucose intolerance in the female pSENP1-KO mice (Supplementary Fig. 2A–F).

A previous study showed that increasing SUMOylation protects from oxidative stress and preserves islet mass (13). Following HFD, we found no differences in  $\beta$ -cell mass, islet number, and islet size in either male (Fig. 3A) or female (Supplementary Fig. 3) pSENP1-KO mice compared with controls. Since OGTT, but not IPGTT, showed impairment in pSENP1-KO mice after HFD, this prompted us to examine the response of islets from these mice to incretin signaling. Single  $\beta$ -cells from pSENP1-KO mice fed HFD showed lower exocytotic responses, and this was more obvious in the presence of the GLP-1 receptor agonist Ex4 (10 nmol/L) or GIP (100 nmol/L) (Fig. 3B). Furthermore, voltage-dependent Ca<sup>2+</sup> currents were similar between pSENP1-WT and -KO  $\beta$ -cells (Fig. 3C). Although incretin receptor activation still increased insulin secretion from pSENP1-KO islets, the secretory response to glucose, Ex4, and GIP remained much lower in islets from HFD-fed pSENP1-KO mice compared with islets from pSENP1-WT littermates (Fig. 3D–F).

### Loss of Islet SENP1 Impairs Glucagon Secretion

With the Pdx1 promoter as the driver of Cre expression, loss of SENP1 will not be restricted to  $\beta$ -cells (28) (Fig. 4A). Indeed, *Senp1* was  $\sim$ 80% lost in the proximal intestine and absent from islets of pSENP1-KO mice (Fig. 4B), suggesting that oral glucose tolerance might be impacted by deletion of SENP1 from incretin-producing intestinal cells or glucagon-producing  $\alpha$ -cells. However, total plasma GLP-1 and GIP levels during an oral glucose challenge were similar between pSENP1-WT and -KO mice on either chow diet (CD) or HFD (Fig. 4C and D). Fasting plasma glucagon appears decreased in the pSENP1-KO, and this is significant after HFD (Fig. 4E). In vitro glucagon secretion from pSENP1-KO islets is reduced compared with control littermates (Fig. 4F and G), including at

responses ( $n = 8, 6,$  and  $5$  mice) (J). Data are mean  $\pm$  SEM and were compared using one-way or two-way ANOVA followed by Bonferroni posttest. \* $P < 0.05$ , \*\*\* $P < 0.001$  between pSENP1-WT and -KO; # $P < 0.05$  between pSENP1-HET and pSENP1-WT; \$ $P < 0.05$ , \$\$ $P < 0.01$  between pSENP1-HET and pSENP1-KO, unless otherwise indicated. AUC, area under the curve; IB, immunoblotting.

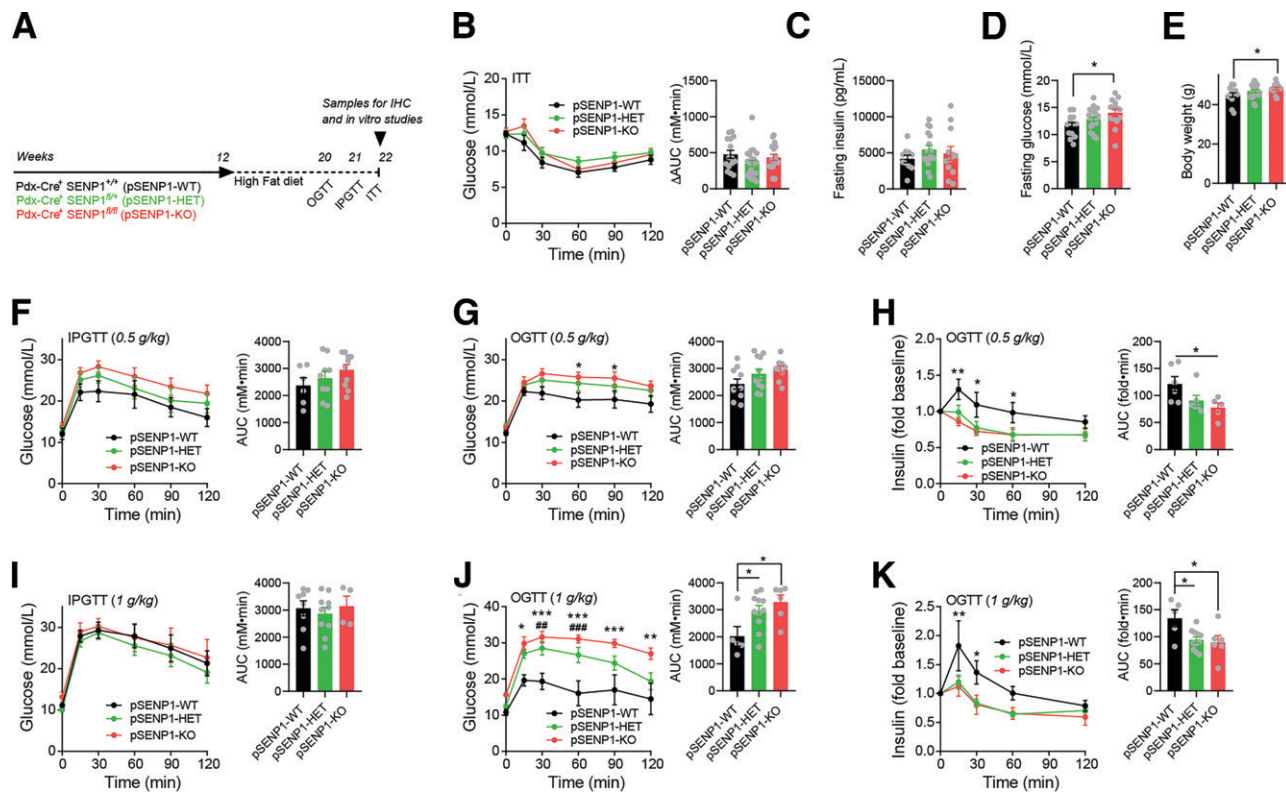


**Figure 2**—Selective worsening of oral glucose tolerance in pSEN1-KO mice after high-fat feeding. **A**: Schematic diagram of experiments on HFD. **B–E**: ITT, fasting insulin, fasting glucose, and body weight of male pSEN1-WT, -HET, and -KO mice on HFD ( $n = 15, 22,$  and  $17$  mice [**B**];  $n = 10, 17,$  and  $12$  mice [**C**];  $n = 13, 21,$  and  $14$  mice [**D**];  $n = 14, 23,$  and  $14$  mice [**E**]). **F**: IPGTT with  $0.5$  g/kg dextrose in male pSEN1-WT, -HET, and -KO mice after HFD ( $n = 6, 9,$  and  $10$  mice). **G** and **H**: OGTT ( $0.5$  g/kg dextrose) of male pSEN1-WT, -HET, and -KO mice after HFD ( $n = 10, 12,$  and  $9$  mice) (**G**) and associated plasma insulin responses ( $n = 6, 6,$  and  $5$  mice) (**H**). **I**: IPGTT with  $1$  g/kg dextrose in male pSEN1-WT, -HET, and -KO mice after HFD ( $n = 8, 10,$  and  $4$  mice). **J** and **K**: OGTT ( $1$  g/kg dextrose) of male pSEN1-WT, -HET, and -KO mice after HFD ( $n = 5, 11,$  and  $6$  mice) (**J**) and associated plasma insulin responses ( $n = 5, 11,$  and  $6$  mice) (**K**). Data are mean  $\pm$  SEM and were compared using Student  $t$  test or one-way or two-way ANOVA followed by Bonferroni posttest.  $*P < 0.05,$   $**P < 0.01,$   $***P < 0.001$  between pSEN1-WT and pSEN1-KO;  $##P < 0.01,$   $###P < 0.001$  between pSEN1-HET and pSEN1-WT. AUC, area under the curve; IHC, immunohistochemistry.

low glucose and in response to GIP alone (29) or with alanine, which we used together to potently activate  $\alpha$ -cells (30). Similar results were observed from islets of pSEN1-KO mice following HFD (data not shown). Although GIP-dependent  $\alpha$ -to- $\beta$ -cell communication primarily impacts the incretin response to a mixed meal, rather than to oral glucose (31), an overall reduction in intra-islet glucagon could reduce insulin secretion by lowering  $\beta$ -cell cAMP tone (26). We wanted to focus on the role for  $\beta$ -cell SENP1 and so generated  $\beta$ SEN1-KO mice (Fig. 4A). Approximately 80% of *Senp1* was lost in islets from  $\beta$ SEN1-KO but was unaffected in other tissues (Fig. 4H), fasting plasma glucagon is not decreased in  $\beta$ SEN1-KO mice on CD or HFD (Fig. 4I), and in vitro glucagon secretion from  $\beta$ SEN1-KO islets was not different from littermate controls (Fig. 4J and K).

**$\beta$ -Cell-Specific Deletion of SENP1 Leads to Worsened Oral Glucose Tolerance After HFD**

We observed no differences in insulin tolerance, fasting insulin, fasting glucose, and body weight in these mice on

CD or HFD (Fig. 5A and B and Supplementary Figs. 4 and 5). Both oral and IP glucose tolerance were similar in  $\beta$ SEN1-KO and WT littermates on CD in both males (Fig. 5C and D) and females (Supplementary Fig. 5D and E). After HFD, male  $\beta$ SEN1-KO mice were more glucose intolerant than  $\beta$ SEN1-WT littermates to oral (Fig. 5E) but not IP (Fig. 5G) glucose. Plasma insulin responses to oral glucose were impaired (Fig. 5F) but not in response to IP glucose (Fig. 5H). Similar, but less striking, differences were observed in females (Supplementary Fig. 5G–K). We found no difference in  $\beta$ -cell mass, islet number, or islet size in  $\beta$ SEN1-KO mice compared with littermate controls (Supplementary Fig. 6A–D) and confirmed impaired single- $\beta$ -cell exocytosis (Fig. 6A) with no significant difference in  $Ca^{2+}$  currents (Fig. 6B). Glucose-stimulated insulin secretion from islets of chow-fed  $\beta$ SEN1-KO mice was reduced (Fig. 6C). After HFD, insulin secretion from islets of  $\beta$ SEN1-KO mice and littermate controls was impaired to the same degree (Fig. 6D). However, insulin secretion from HFD  $\beta$ SEN1-WT islets was potentiated

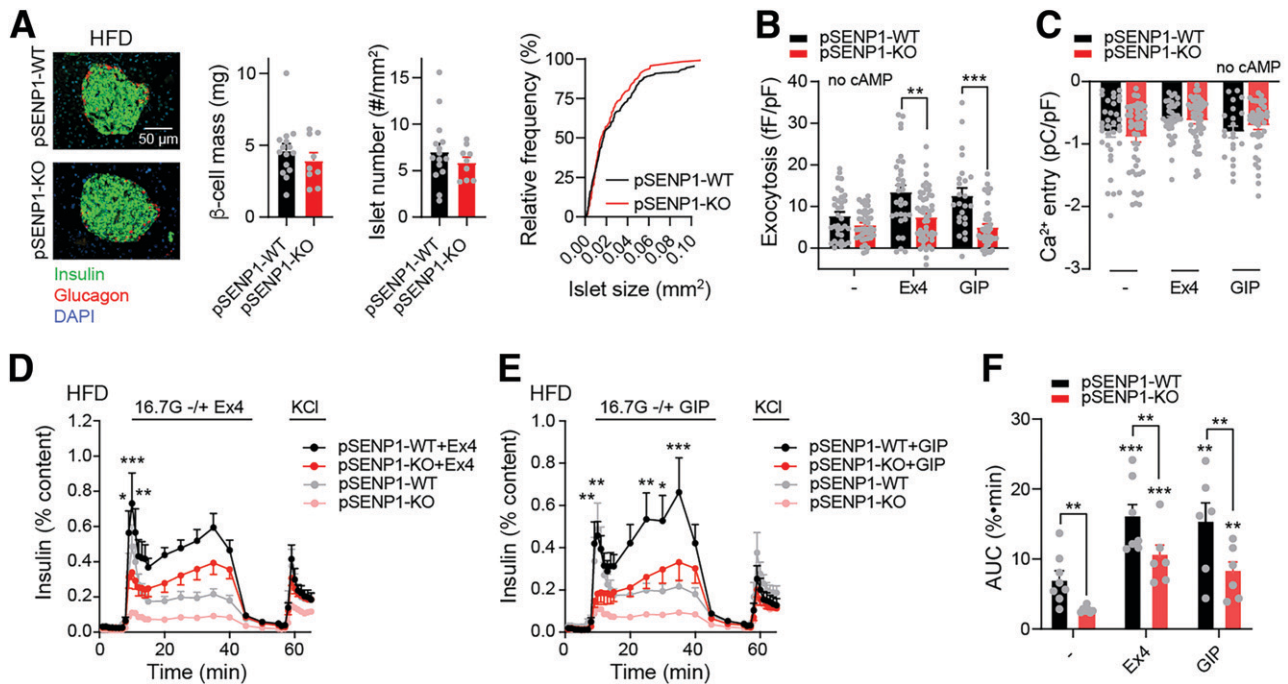


**Figure 3**—Impaired insulin secretion and exocytosis to glucose and incretins from male pSENP1-KO mice following HFD. **A**: Representative immunostaining and quantification of  $\beta$ -cell mass, islet number, and islet size distribution in male pSENP1-WT ( $n = 5$  mice, 15 sections, and 220 islets) and pSENP1-KO ( $n = 3$  mice, 9 sections, and 116 islets) pancreas following HFD. **B**:  $\beta$ -Cell exocytosis, following HFD, elicited by a series of 500-ms membrane depolarization from  $-70$  mV to  $0$  mmol/L in the presence of  $5$  mmol/L glucose alone and together with Ex4 ( $10$  nmol/L) or GIP ( $100$  nmol/L) ( $n = 24$ – $42$  cells from 3–5 pairs of male mice). cAMP was omitted from the pipette solution. **C**: Average integrated Ca<sup>2+</sup> currents elicited by a single 500-ms membrane depolarization from  $-70$  mV to  $0$  mmol/L at  $5$  mmol/L glucose or with Ex4 or GIP ( $n = 21$ – $48$  cells). cAMP was omitted in pipette solution. **D** and **E**: Insulin secretion from male pSENP1-WT and -KO islets following HFD in response to glucose alone ( $n = 8$  and  $6$ ) (**D** and **E**) or together with Ex4 ( $10$  nmol/L) ( $n = 7$  and  $6$ ) (**D**) or GIP ( $100$  nmol/L) ( $n = 6$  and  $6$ ) (**E**). **F**: Area under the curve (AUC) during the glucose stimulation from **D** and **E**. Data are mean  $\pm$  SEM and were compared using Student *t* test or one-way or two-way ANOVA followed by Bonferroni posttest. \* $P < 0.05$ , \*\* $P < 0.01$ , \*\*\* $P < 0.001$  compared with the control condition. In panels **D** and **E**, we show significance comparing the pSENP1-WT and -KO in the presence of Ex4 or GIP only.

to a greater degree by Ex4 and GIP than from  $\beta$ SENP1-KO islets (Fig. 6D–F). Consistently, Ex4 and GIP were unable to increase exocytosis to the same extent from  $\beta$ -cells of HFD  $\beta$ SENP1-KO mice compared with littermate controls (Fig. 6G), independent of any changes in Ca<sup>2+</sup> currents (Supplementary Fig. 7A).

Although SUMOylation may inhibit GLP-1 receptor activity (32,33), we found no difference in the cAMP response to Ex4 or GIP between  $\beta$ SENP1-WT and -KO islets expressing the  $\beta$ -cell-specific cAMP sensor (Fig. 6H and I and Supplementary Fig. 8). Even though our experiments include cAMP in the patch pipette, exocytosis from  $\beta$ -cells of  $\beta$ SENP1-KO mice following HFD was still much lower than in littermate controls (Fig. 6J and K). While the cycling period of Ca<sup>2+</sup> oscillations was higher in  $\beta$ SENP1-KO  $\beta$ -cells, the time in the active phase remained the same (Fig. 6L and M), suggesting that SENP1 acts downstream of the Ca<sup>2+</sup> response and that the increased cycling period may be secondary to the reduced workload (ATP hydrolysis) in the  $\beta$ SENP1-KO  $\beta$ -cells because of loss of exocytosis (34). Ex4 and GIP maintained their effect on Ca<sup>2+</sup> responses (Fig. 6L and M and Supplementary Fig. 7D and E), and  $\beta$ SENP1-KO

islets exhibited impaired oleate-stimulated and glutamine/leucine-stimulated insulin secretion (Supplementary Fig. 7B and C). This all points to a mechanism downstream of cAMP and Ca<sup>2+</sup> responses (9,10,35).

## DISCUSSION

We aimed to investigate the role of the deSUMOylating enzyme SENP1 within the  $\beta$ -cell following HFD-induced metabolic stress. In two models, we confirmed that loss of  $\beta$ -cell SENP1 results in impaired exocytosis and reduced insulin secretion, consistent with the SUMOylation-dependent inhibition of insulin secretion in insulinoma cells and human and mouse  $\beta$ -cells (7,9–11,13). DeSUMOylation, likely of multiple targets (6), is an important mechanism that facilitates insulin secretion. In vivo, overexpression of the SUMO-conjugating enzyme Ubc9 within  $\beta$ -cells leads to an obvious IP glucose intolerance (13). While we see impaired insulin secretion, we do not find robust glucose intolerance in young chow-fed mice following islet or  $\beta$ -cell SENP1 KO. Thus, insulin secretion may not be sufficiently limited in vivo to

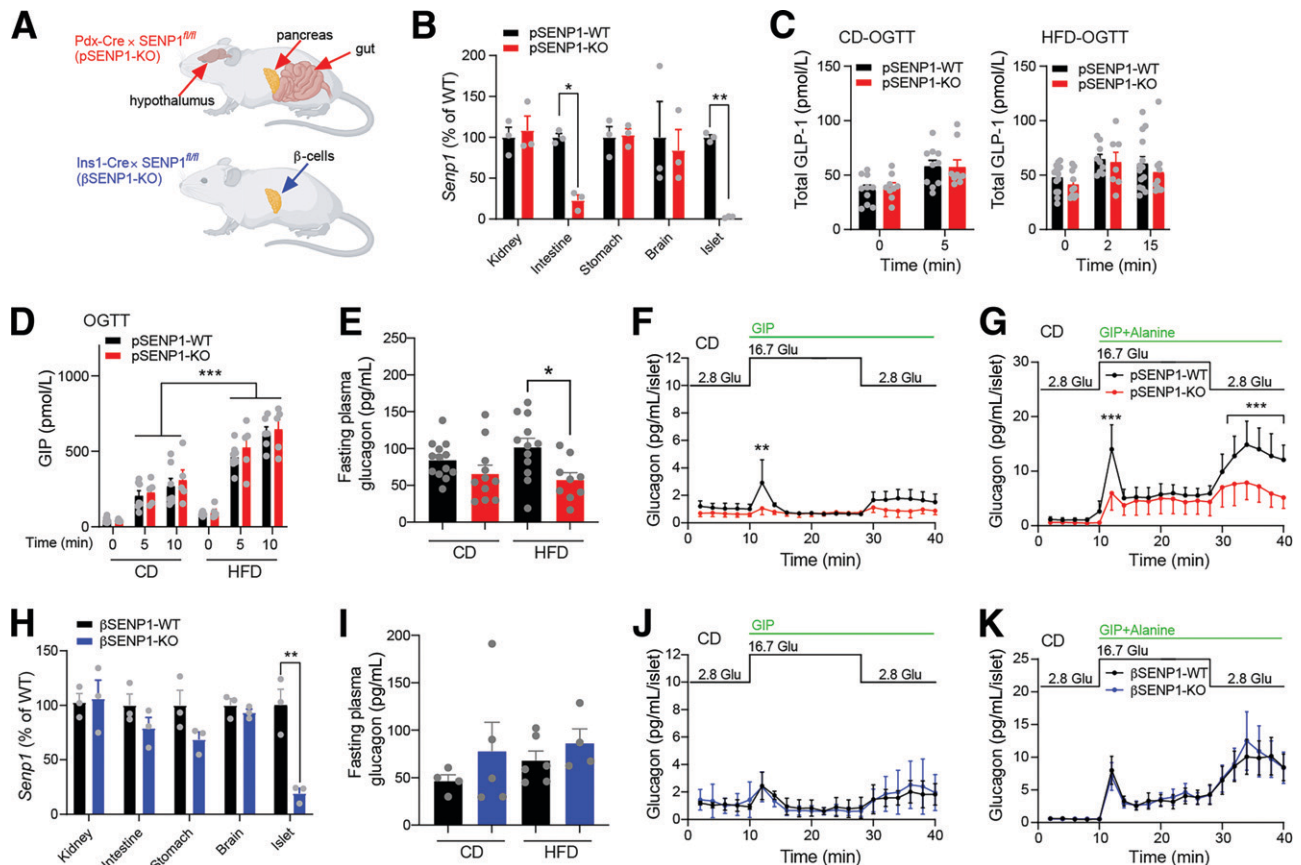


**Figure 4**—Generation of a  $\beta$ SEN1-KO. **A**: Expected tissue selectivity of SENP1 KO in the pSEN1-KO and  $\beta$ SEN1-KO mice. **B**: qPCR of *Senp1* expression in tissues from pSEN1-WT and -KO mice ( $n = 3$  and  $3$ ). **C**: Oral glucose-stimulated total plasma GLP-1 in CD ( $n = 10$  and  $9$ ) and HFD ( $n = 10$  and  $9$ ) mice. **D**: Oral glucose-stimulated plasma GIP in CD and HFD mice ( $n = 5$ – $9$  mice). **E**: Fasting plasma glucagon from pSEN1-WT and -KO mice fed CD or HFD ( $n = 13, 11, 12$ , and  $9$ ). **F** and **G**: Glucagon secretion at indicated glucose levels in the presence of GIP ( $n = 3$  and  $3$ ) or GIP + alanine from islets of pSEN1-WT and -KO mice on CD ( $n = 4$  and  $4$ ) (**F**) or GIP + alanine from islets of pSEN1-WT and -KO mice on CD ( $n = 4$  and  $4$ ) (**G**). **H**: qPCR of *Senp1* expression in tissues from  $\beta$ SEN1-WT and -KO mice ( $n = 3$  and  $3$ ). **I**: Fasting plasma glucagon from  $\beta$ SEN1-WT and -KO mice fed CD or HFD ( $n = 4, 5, 6$ , and  $4$ ). **J** and **K**: Glucagon secretion at indicated glucose level in the presence of GIP ( $n = 4$  and  $4$ ) (**J**) or GIP + alanine from islets of  $\beta$ SEN1-WT and -KO mice on CD ( $n = 5$  and  $4$ ) (**K**). Data from male and female islets were combined and are mean  $\pm$  SEM and were compared using Student *t* test or one-way or two-way ANOVA followed by Bonferroni posttest. \* $P < 0.05$ , \*\* $P < 0.01$ , \*\*\* $P < 0.001$  between pSEN1-WT and pSEN1-KO or between  $\beta$ SEN1-WT and  $\beta$ SEN1-KO. Glu, glucose.

consistently impact glucose homeostasis in the absence of a stressor. At present, we also cannot rule out potential compensatory mechanisms in vivo, such as increased insulin sensitivity, that might be difficult to detect in our ITTs. Nonetheless, high-fat feeding revealed the importance SENP1-dependent insulin secretion in the maintenance of glucose homeostasis.

A worsening of HFD-induced glucose intolerance in both the pSEN1-KO and the  $\beta$ SEN1-KO mice was observed selectively in response to oral, but not IP, glucose. This suggests an important interaction with the incretin response, which is upregulated in HFD (36–38) consistent with the enhanced GIP response we observed. Recent work suggested an important interaction among incretin responses, glucagon secretion, and insulin release (39). GIP-induced glucagon secretion supports insulin secretion following a mixed meal (26,40–42) but does not

likely contribute in the response to oral glucose alone (31). Thus, the reduced glucagon response to GIP + alanine in the pSEN1-KO islets used here as a strong stimulus of  $\alpha$ -cell function likely does not contribute to worsened oral glucose intolerance. It is possible, however, that reduced glucagon “tone” in the pSEN1-KO islets could impact insulin secretion by lowering baseline  $\beta$ -cell cAMP (26) and contribute to the lower insulin response in the pSEN1-KO compared with the  $\beta$ SEN1-KO model. Regardless, the observation that HFD-induced oral glucose intolerance persists in the  $\beta$ SEN1-KO model suggests that loss of SENP1 in the  $\beta$ -cell, rather than in  $\alpha$ -cells or in the intestine, is primarily responsible for the impaired oral glucose tolerance following HFD.

But why is IP glucose tolerance after HFD not worsened in these models, particularly given the role for SENP1 in glucose-stimulated insulin secretion? In  $\beta$ SEN1-KO, this

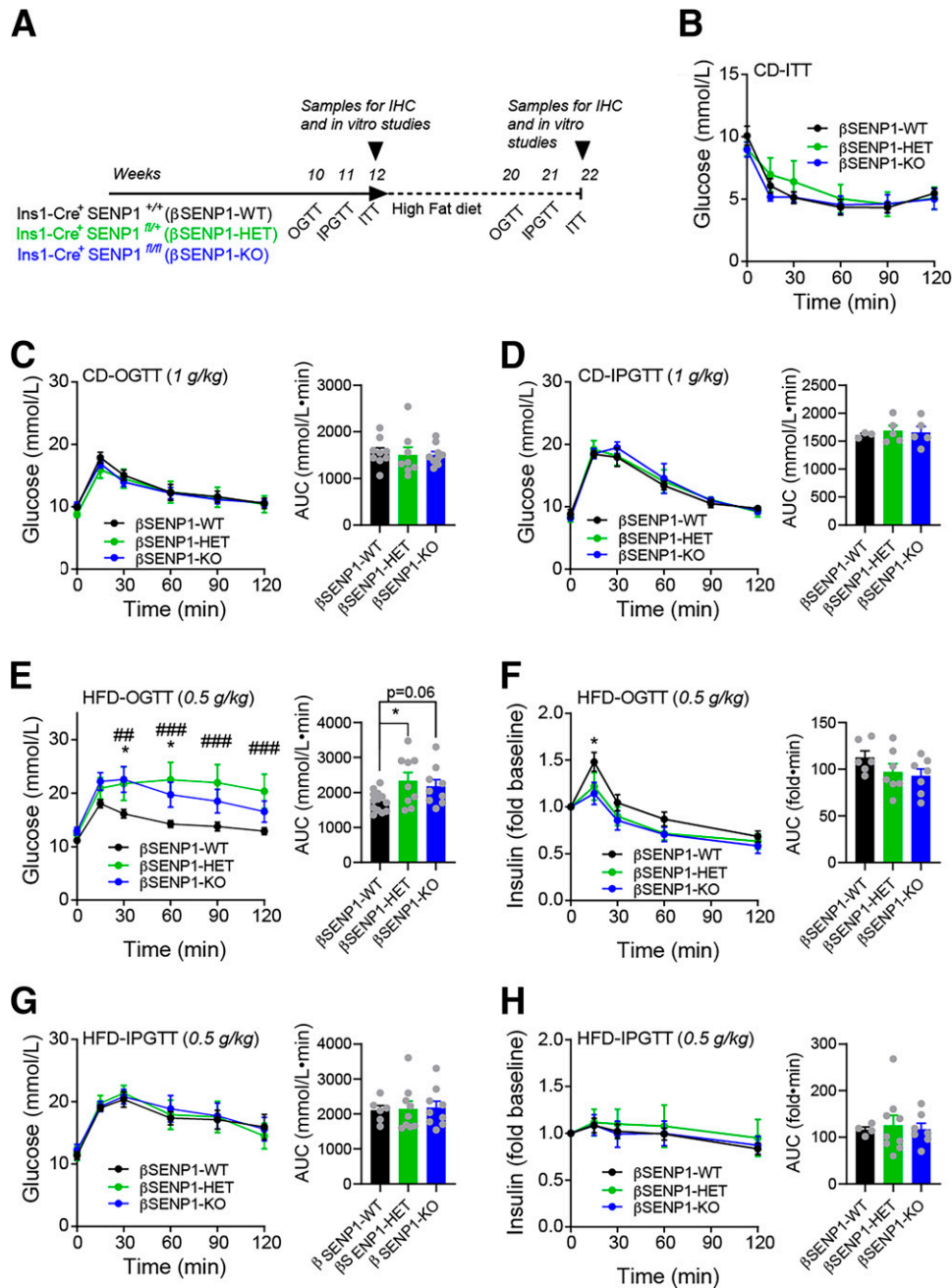


**Figure 5**— $\beta$ SEN1-KO worsens oral, but not IP, glucose tolerance following HFD. **A**: Schematic diagram of experiments on CD and HFD. **B**: ITT of male  $\beta$ SEN1-WT, -HET, and -KO mice on CD ( $n = 6, 6,$  and  $6$  mice). **C**: OGTT of male  $\beta$ SEN1-WT, -HET, and -KO mice on CD ( $n = 9, 8,$  and  $9$  mice). **D**: IPGTT of male  $\beta$ SEN1-WT, -HET, and -KO mice on CD ( $n = 3, 5,$  and  $5$  mice). **E** and **F**: OGTT of male  $\beta$ SEN1-WT, -HET, and -KO mice following HFD ( $n = 13, 9,$  and  $9$  mice) (**E**) and associated plasma insulin responses ( $n = 6, 7,$  and  $7$  mice) (**F**). **G** and **H**: IPGTT (0.5 g/kg) of male  $\beta$ SEN1-WT, -HET, and -KO mice after HFD ( $n = 6, 9,$  and  $9$  mice) (**G**) and associated plasma insulin responses ( $n = 4, 9,$  and  $7$  mice) (**H**). Data are mean  $\pm$  SEM and were compared using one-way or two-way ANOVA followed by Bonferroni posttest. \* $P < 0.05$  between  $\beta$ SEN1-WT and  $\beta$ SEN1-KO; ## $P < 0.01$ , ### $P < 0.001$  between  $\beta$ SEN1-HET and  $\beta$ SEN1-WT, unless otherwise indicated. AUC, area under the curve; IHC, immunohistochemistry.

is easier to explain since glucose-stimulated insulin secretion is similarly impaired after HFD in both KO and WT islets. In  $\beta$ SEN1-KO, a lower glucose-stimulated insulin secretion in vitro after HFD has only a small impact, if any, to worsen IP glucose intolerance. The reasons for this

are likely twofold. First, after the 8-week HFD, insulin secretion from the  $\beta$ SEN1-WT islets is already impaired (a peak of  $\sim 0.4\%$  of content as in Fig. 3D and E) compared with chow-fed WT mice in our hands (peak of  $\sim 1.5\%$  as in Fig. 6C or elsewhere [7]). The additional reduction of

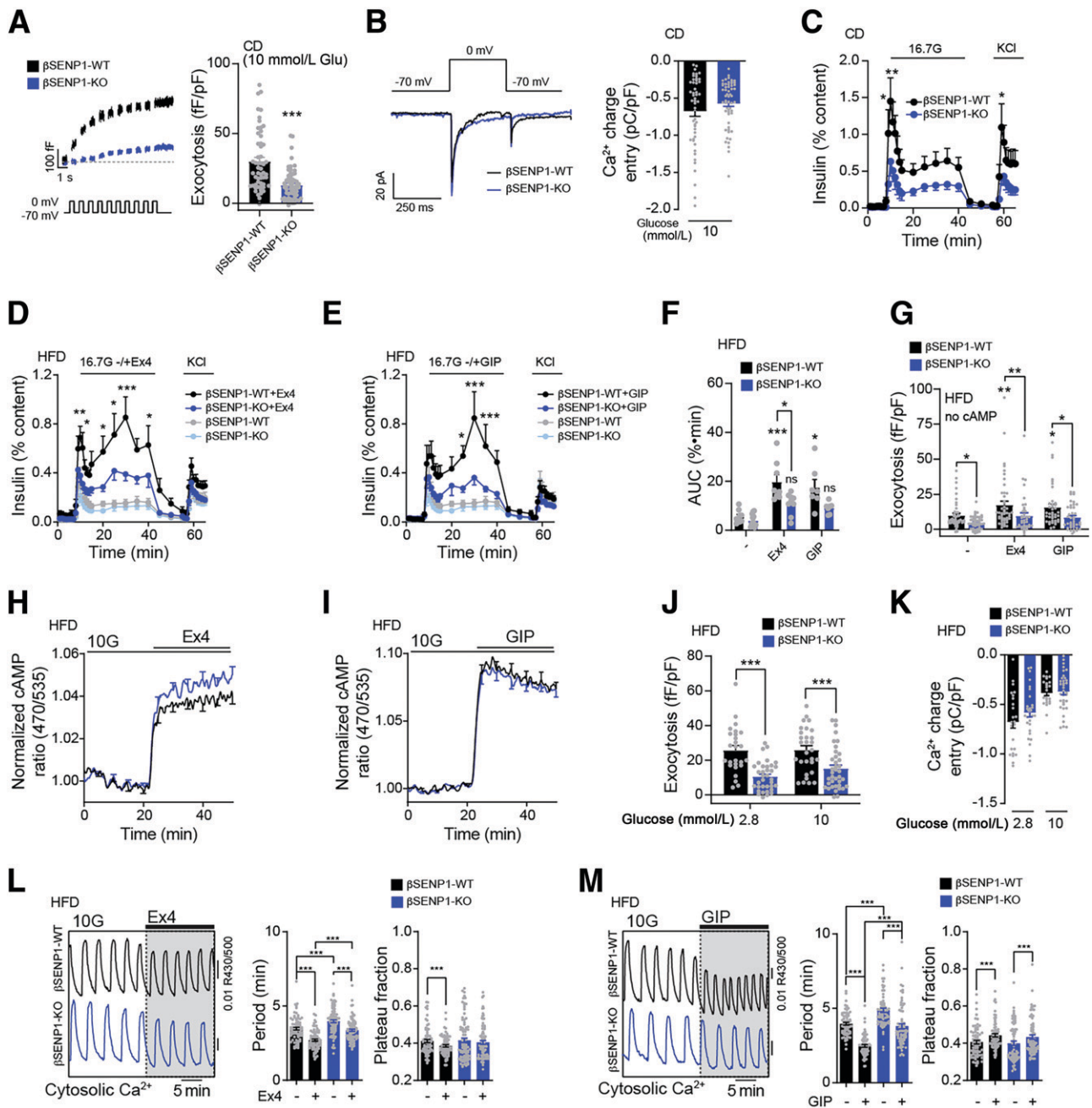


**Figure 6**—Impaired insulin secretion and exocytosis to glucose and incretins from  $\beta$ SENP1-KO islets following HFD. **A:** Representative traces (left) and averaged exocytosis elicited by a series of 500-ms membrane depolarizations from -70 to 0 mV in  $\beta$ -cells from male  $\beta$ SENP1-WT and -KO mice on CD at 10 mmol/L glucose ( $n = 55$  and  $61$  cells from  $5$  and  $7$  mice). The pipette solution included  $0.1$  mmol/L cAMP. **B:** Representative  $Ca^{2+}$  current traces and average integrated  $Ca^{2+}$  entry of  $\beta$ -cell elicited by a single 500-ms membrane depolarization from -70 to 0 mV at 10 mmol/L glucose ( $n = 51$  and  $57$  cells). The pipette solution included  $0.1$  mmol/L cAMP. **C:** Insulin secretion from male  $\beta$ SENP1-WT and -KO islets from mice on CD in response to glucose alone ( $n = 8$  and  $7$ ). **D** and **F:** Side-by-side insulin secretion from  $\beta$ SENP1-WT and -KO islets from male mice following HFD in response to glucose alone ( $n = 9$  and  $12$ ) (**D** and **F**) or together with Ex4 ( $10$  nmol/L) ( $n = 8$  and  $9$ ) (**D**) or GIP ( $100$  nmol/L) ( $n = 7$  and  $7$ ) (**E**) and respective area under the curve (AUC) during the glucose stimulation (**F**). **G:** Exocytosis in  $\beta$ -cells of male  $\beta$ SENP1-WT and -KO mice, following HFD, elicited by a series of 500-ms membrane depolarization from -70 to 0 mV at  $5$  mmol/L glucose alone or with Ex4 ( $10$  nmol/L) or GIP ( $100$  nmol/L) ( $n = 44, 46, 47, 38, 40,$  and  $41$  cells from  $5$  mice per group). cAMP  $0.1$  mmol/L was omitted from pipette solution. **H** and **I:** The cAMP response at  $10$  mmol/L glucose to Ex4 ( $10$  nmol/L) ( $n = 4$  pairs of mice,  $68$  and  $74$  islets) (**H**) or GIP ( $100$  nmol/L) ( $n = 4$  pairs of mice,  $73$  and  $88$  islets) (**I**). **J:** Exocytosis in  $\beta$ -cells of male  $\beta$ SENP1-WT and -KO mice following HFD at  $2.8$  and  $10$  mmol/L glucose, with  $0.1$  mmol/L cAMP included in the pipette solution ( $n = 26, 35, 29,$  and  $38$  cells from  $3, 4, 3,$  and  $4$  mice). **K:** Average integrated  $Ca^{2+}$  charge entry during voltage-dependent  $Ca^{2+}$  currents elicited from  $\beta$ -cells by a single 500-ms membrane depolarization from -70 to 0 mV at  $2.8$  and  $10$  mmol/L glucose ( $n = 26, 30, 30,$  and  $38$  cells from  $3, 4, 3,$  and  $4$  mice). The pipette solution included  $0.1$  mmol/L cAMP. **L** and **M:** Representative  $Ca^{2+}$  responses (left), oscillation period, and  $Ca^{2+}$  plateau fraction at  $10$  mmol/L glucose to Ex4 ( $n = 4$  pairs of mice,  $73$  and  $88$  cells) (**L**) and to GIP ( $n = 4$  pairs of mice,  $68$  and  $74$  cells) (**M**). Data are mean  $\pm$  SEM and were compared using Student  $t$  test or one-way or two-way ANOVA followed by Bonferroni post-test. \* $P < 0.05$ , \*\* $P < 0.01$ , \*\*\* $P < 0.001$  between  $\beta$ SENP1-WT and -KO under the same condition.

glucose-stimulated secretion may be insufficient to worsen an already-impaired IP glucose tolerance. Second, plasma glucose clearance following IP administration is more dependent on insulin-independent mechanisms than glucose through the oral route (43). Glucose effectiveness, the ability of glucose to promote its own insulin-independent clearance, contributes two-thirds of clearance following IP glucose in mice (44), and this proportion increases substantially following high-fat feeding (45,46). This, coupled with upregulation of incretin responses upon high-fat feeding, may explain why we see a stronger effect of islet SENP1 KO on oral glucose tolerance in our HFD mice.

Although SUMOylation is suggested to reduce GLP-1 receptor activity (32,33), cAMP and  $\text{Ca}^{2+}$  responses to Ex4 and GIP were similar between  $\beta$ SENP1-WT and -KO islets. Therefore, SENP1 does not appear to control incretin receptor activity directly, although it is possible that other SUMO proteases (47) may be key determinants of upstream incretin signaling. Also,  $\beta$ -cells lacking SENP1 show decreased exocytosis, even though most patch clamp experiments included high cAMP in the pipette solution, which should bypass the need for incretin receptor activation. This suggests that the impaired response upon loss of SENP1 resides downstream of receptor signaling and cAMP, although it could be possible that effectors such as cAMP-dependent protein kinase or exchange protein directly activated by cAMP are directly impacted by loss of SENP1. The observation that insulin secretion from  $\beta$ SENP1-KO islets was also impaired upon fatty acid or amino acid stimulation suggests that SENP1 acts far downstream in the regulation of insulin granule fusion. Although we see reduced  $\text{Ca}^{2+}$  oscillation frequency in the  $\beta$ SENP1-KO, this is likely secondary to the reduced workload resulting from a loss of exocytosis (34). It seems, therefore, that SENP1 is required to ensure the availability of insulin granules on which cAMP-dependent signals act or that these converge on common exocytotic protein targets, such as synaptotagmin VII, shared by other metabolic pathways (9,35).

As such, we do not believe that SENP1 activity “mediates” incretin signaling but rather serves an important role in maintaining, or augmenting, the pool of release-ready insulin granules on which incretins ultimately act. Interestingly, the activity of SENP1 is linked to metabolism and the mitochondrial export of reducing equivalents (6,7) to mediate an amplification of insulin secretion. SUMOylation blocks granule fusion at a very distal step in the secretory pathway, producing a “traffic jam” of insulin granules at the plasma membrane (9). Thus, SENP1 acts to maintain, or perhaps amplify, the availability of secretory granules for subsequent release whether in response to glucose, incretins, or other stimuli. This suggests that a glucose-dependent effect to enhance the secretory granule pool will augment the secretory response to incretins. Indeed, the ability of

glucose to facilitate  $\beta$ -cell exocytosis is correlated with Ex4-dependent insulin secretion from human islets (5).

The SENP1 pathway itself may be impaired by HFD possibly because of inactivation of SENP1 by oxidative stress (48) and similar to what occurs in islets from human donors with T2D (7). The export of mitochondrial reducing equivalents activates SENP1 by reducing a thiol group through a redox relay involving NADPH and reduction of glutathione (7,48). On the other hand,  $\text{H}_2\text{O}_2$ , which can oxidize and inactivate SENP1 (8), is also produced from NADPH through NOX4, and this is also required for glucose-stimulated insulin secretion (49,50). It remains unclear how SENP1 may evade  $\text{H}_2\text{O}_2$ -induced inactivation and compete with NOX4 for NADPH. One possibility may involve either spatial or temporal compartmentalization. SENP1 potentiates insulin secretion by modulating exocytotic proteins (6,9–11), while NOX4-induced  $\text{H}_2\text{O}_2$  primarily acts through  $\text{K}_{\text{ATP}}$  channel inhibition (49). Here, excessive oxidative stress induced by HFD could lead to basal hyperinsulinemia and defective glucose-stimulated insulin secretion (51), as occurs in islets from donors with impaired glucose tolerance or T2D (52). Indeed, NOX4-induced islet  $\text{H}_2\text{O}_2$  may drive  $\beta$ -cell dysfunction and glucose intolerance after HFD (53), and it is interesting to speculate that overproduction of  $\text{H}_2\text{O}_2$  could spill over and limit SENP1 activity and increase SUMOylation. While inhibition or loss of SENP1 may protect against  $\beta$ -cell apoptosis (13), it comes at the cost of robust incretin-induced insulin secretion in the face of metabolic stressors.

---

**Acknowledgments.** The authors thank Dr. Edward Yeh (University of Arkansas) who originally provided the SENP1<sup>fl/fl</sup> mice, Dr. Jon Campbell (Duke University) and Dr. Sam Virtue (Cambridge) for many helpful discussions, and Emily Knuth (Merrins Laboratory, University of Wisconsin–Madison) for technical assistance.

**Funding.** This work was funded by a Canadian Institutes of Health Research Foundation Grant (148451 to P.E.M.). H.L. was supported by a Sino-Canadian Studentship from Shantou University. S.L.L. and M.J.M. were supported by National Institutes of Health grants F31-DK-126403 and R01-DK-113103 and R01-DK-127637, respectively. Y.J. was supported by a University of Alberta Office of the Provost and Vice President (Academic) Summer Studentship. P.E.M. holds the Canada Research Chair in Islet Biology.

**Duality of Interest.** No potential conflicts of interest relevant to this article were reported.

**Author Contributions.** H.L., N.S., A.F.S., K.S., M.F., T.A.A., S.L.L., Y.J., A.B., and Y.W.W. researched and analyzed data. H.L., J.E.M.F., M.J.M., J.B., and P.E.M. designed the studies. H.L. and P.E.M. wrote the manuscript. All authors edited and approved of the final version. P.E.M. is the guarantor of the work and, as such, had full access to all the data in the study and takes responsibility for the integrity of the data and the accuracy of the data analysis.

## References

1. Kalwat MA, Cobb MH. Mechanisms of the amplifying pathway of insulin secretion in the  $\beta$  cell. *Pharmacol Ther* 2017;179:17–30

2. Gheni G, Ogura M, Iwasaki M, et al. Glutamate acts as a key signal linking glucose metabolism to incretin/cAMP action to amplify insulin secretion. *Cell Rep* 2014;9:661–673
3. Campbell JE, Drucker DJ. Pharmacology, physiology, and mechanisms of incretin hormone action. *Cell Metab* 2013;17:819–837
4. Oduori OS, Murao N, Shimomura K, et al. Gs/Gq signaling switch in  $\beta$  cells defines incretin effectiveness in diabetes. *J Clin Invest* 2020;130:6639–6655
5. Ferdaoussi M, Smith N, Lin H, et al. Improved glucose tolerance with DPPIV inhibition requires  $\beta$ -cell SENP1 amplification of glucose-stimulated insulin secretion. *Physiol Rep* 2020;8:e14420
6. Ferdaoussi M, MacDonald PE. Toward connecting metabolism to the exocytotic site. *Trends Cell Biol* 2017;27:163–171
7. Ferdaoussi M, Dai X, Jensen MV, et al. Isocitrate-to-SENP1 signaling amplifies insulin secretion and rescues dysfunctional  $\beta$  cells. *J Clin Invest* 2015;125:3847–3860
8. Vergari E, Plummer G, Dai X, MacDonald PE. DeSUMOylation controls insulin exocytosis in response to metabolic signals. *Biomolecules* 2012;2:269–281
9. Dai X-Q, Plummer G, Casimir M, et al. SUMOylation regulates insulin exocytosis downstream of secretory granule docking in rodents and humans. *Diabetes* 2011;60:838–847
10. Ferdaoussi M, Fu J, Dai X, et al. SUMOylation and calcium control syntaxin-1A and secretagogin sequestration by tomosyn to regulate insulin exocytosis in human  $\beta$  cells. *Sci Rep* 2017;7:248
11. Davey JS, Carmichael RE, Craig TJ. Protein SUMOylation regulates insulin secretion at multiple stages. *Sci Rep* 2019;9:2895
12. Hajmirle C, Ferdaoussi M, Plummer G, et al. SUMOylation protects against IL-1 $\beta$ -induced apoptosis in INS-1 832/13 cells and human islets. *Am J Physiol Endocrinol Metab* 2014;307:E664–E673
13. He X, Lai Q, Chen C, et al. Both conditional ablation and overexpression of E2 SUMO-conjugating enzyme (UBC9) in mouse pancreatic beta cells result in impaired beta cell function. *Diabetologia* 2018;61:881–895
14. MacDonald PE. A post-translational balancing act: the good and the bad of SUMOylation in pancreatic islets. *Diabetologia* 2018;61:775–779
15. Thorens B, Tarussio D, Maestro MA, Rovira M, Heikkilä E, Ferrer J. Ins1(Cre) knock-in mice for beta cell-specific gene recombination. *Diabetologia* 2015;58:558–565
16. Smith N, Ferdaoussi M, Lin H, MacDonald PE. Oral glucose tolerance test in mouse, 2020. Accessed 15 April 2020. Available from <https://doi.org/10.17504/protocols.io.ujjeukn>.
17. Smith N, Ferdaoussi M, Lin H, MacDonald PE. IP glucose tolerance test in mouse, 2020. Accessed 15 April 2020. Available from <https://doi.org/10.17504/protocols.io.wxhffj6>
18. Smith N, Ferdaoussi M, Lin H, MacDonald PE. Insulin tolerance test in mouse, 2020. Accessed 15 April 2020. Available from <https://doi.org/10.17504/protocols.io.wxjffkn>
19. Spigelman AF. Static glucose-stimulated insulin secretion (GSIS) protocol - human islets V.2, 2019. Accessed 11 January 2019. Available from <https://doi.org/10.17504/protocols.io.wy4ffyw>
20. Smith N, Spigelman AF, Lin H, MacDonald PE. Mouse Pancreatic Islet Isolation, 2020. Accessed 15 April 2020. Available from <https://doi.org/10.17504/protocols.io.sqaedse>
21. Ferdaoussi M, Bergeron V, Zarrouki B, et al. G protein-coupled receptor (GPR)40-dependent potentiation of insulin secretion in mouse islets is mediated by protein kinase D1. *Diabetologia* 2012;55:2682–2692
22. Spigelman AF, Ferdaoussi M, MacDonald PE. Complexing sodium oleate for use in insulin secretion, 2021. Accessed 5 May 2021. Available from <https://doi.org/10.17504/protocols.io.buamns6>
23. Spigelman AF, Manning Fox JE, MacDonald PE. Static glucose-stimulated insulin secretion (GSIS) protocol: mouse islets, 2021. Accessed 5 May 2021. Available from <https://doi.org/10.17504/protocols.io.sp7edrn>
24. Zhang Q, Chibalina MV, Bengtsson M, et al. Na<sup>+</sup> current properties in islet  $\alpha$ - and  $\beta$ -cells reflect cell-specific Scn3a and Scn9a expression. *J Physiol* 2014;592:4677–4696. DOI: 10.1113/jphysiol.2014.274209
25. Klarenbeek J, Goedhart J, van Batenburg A, Groenewald D, Jalink K. Fourth-generation EPAC-based FRET sensors for cAMP feature exceptional brightness, photostability and dynamic range: characterization of dedicated sensors for FLIM, for ratiometry and with high affinity. *PLoS One* 2015;10:e0122513
26. Capozzi ME, Svendsen B, Encisco SE, et al.  $\beta$  Cell tone is defined by proglucagon peptides through cAMP signaling. *JCI Insight* 2019;4:126742
27. Pettersson US, Waldén TB, Carlsson P-O, Jansson L, Phillipson M. Female mice are protected against high-fat diet induced metabolic syndrome and increase the regulatory T cell population in adipose tissue. *PLoS One* 2012;7:e46057
28. Magnuson MA, Osipovich AB. Pancreas-specific Cre driver lines and considerations for their prudent use. *Cell Metab* 2013;18:9–20
29. El K, Campbell JE. The role of GIP in  $\alpha$ -cells and glucagon secretion. *Peptides* 2020;125:170213
30. Galsgaard KD, Jepsen SL, Kjeldsen SAS, Pedersen J, Wewer Albrechtsen NJ, Holst JJ. Alanine, arginine, cysteine, and proline, but not glutamine, are substrates for, and acute mediators of, the liver- $\alpha$ -cell axis in female mice. *Am J Physiol Endocrinol Metab* 2020;318:E920–E929
31. El K, Gray SM, Capozzi ME, et al. GIP mediates the incretin effect and glucose tolerance by dual actions on  $\alpha$  cells and  $\beta$  cells. *Sci Adv* 2021;7:eabf1948
32. Rajan S, Torres J, Thompson MS, Phillipson LH. SUMO downregulates GLP-1-stimulated cAMP generation and insulin secretion. *Am J Physiol Endocrinol Metab* 2012;302:E714–E723
33. Rajan S, Dickson LM, Mathew E, et al. Chronic hyperglycemia downregulates GLP-1 receptor signaling in pancreatic  $\beta$ -cells via protein kinase A. *Mol Metab* 2015;4:265–276
34. Lewandowski SL, Cardone RL, Foster HR, et al. Pyruvate kinase controls signal strength in the insulin secretory pathway. *Cell Metab* 2020;32:736–750.e5
35. Wu B, Wei S, Petersen N, et al. Synaptotagmin-7 phosphorylation mediates GLP-1-dependent potentiation of insulin secretion from  $\beta$ -cells. *Proc Natl Acad Sci U S A* 2015;112:9996–10001
36. Gupta D, Jetton TL, LaRock K, et al. Temporal characterization of  $\beta$  cell-adaptive and -maladaptive mechanisms during chronic high-fat feeding in C57BL/6NTac mice. *J Biol Chem* 2017;292:12449–12459
37. Yamane S, Harada N, Inagaki N. Mechanisms of fat-induced gastric inhibitory polypeptide/glucose-dependent insulinotropic polypeptide secretion from K cells. *J Diabetes Investig* 2016;7(Suppl. 1):20–26
38. Ahrén B, Winzell MS, Pacini G. The augmenting effect on insulin secretion by oral versus intravenous glucose is exaggerated by high-fat diet in mice. *J Endocrinol* 2008;197:181–187
39. El K, Capozzi ME, Campbell JE. Repositioning the alpha cell in postprandial metabolism. *Endocrinology* 2020;161:bqaa169
40. Capozzi ME, Wait JB, Koech J, et al. Glucagon lowers glycemia when  $\beta$ -cells are active. *JCI Insight* 2019;5:e129954
41. Zhu L, Dattaray D, Pham J, et al. Intra-islet glucagon signaling is critical for maintaining glucose homeostasis. *JCI Insight* 2019;5:127994
42. Svendsen B, Larsen O, Gabe MBN, et al. Insulin secretion depends on intra-islet glucagon signaling. *Cell Rep* 2018;25:1127–1134.e2
43. Virtue S, Vidal-Puig A. GTTs and ITTs in mice: simple tests, complex answers. *Nat Metab* 2021;3:883–886
44. Pacini G, Thomaseth K, Ahrén B. Contribution to glucose tolerance of insulin-independent vs. insulin-dependent mechanisms in mice. *Am J Physiol Endocrinol Metab* 2001;281:E693–E703
45. Ahrén B, Pacini G. Insufficient islet compensation to insulin resistance vs. reduced glucose effectiveness in glucose-intolerant mice. *Am J Physiol Endocrinol Metab* 2002;283:E738–E744

46. Ahrén B, Pacini G. Glucose effectiveness: lessons from studies on insulin-independent glucose clearance in mice. *J Diabetes Investig* 2021;12:675–685
47. Nayak A, Müller S. SUMO-specific proteases/isopeptidases: SENPs and beyond. *Genome Biol* 2014;15:422
48. Xu Z, Lam LSM, Lam LH, Chau SF, Ng TB, Au SWN. Molecular basis of the redox regulation of SUMO proteases: a protective mechanism of intermolecular disulfide linkage against irreversible sulfhydryl oxidation. *FASEB J* 2008;22:127–137
49. Plecítá-Hlavatá L, Jabůrek M, Holendová B, et al. Glucose-stimulated insulin secretion fundamentally requires H<sub>2</sub>O<sub>2</sub> signaling by NADPH oxidase 4. *Diabetes* 2020;69:1341–1354
50. Leloup C, Tourrel-Cuzin C, Magnan C, et al. Mitochondrial reactive oxygen species are obligatory signals for glucose-induced insulin secretion. *Diabetes* 2009;58:673–681
51. Cohrs CM, Panzer JK, Drotar DM, et al. Dysfunction of persisting  $\beta$  cells is a key feature of early type 2 diabetes pathogenesis. *Cell Rep* 2020;31:107469
52. Sakuraba H, Mizukami H, Yagihashi N, Wada R, Hanyu C, Yagihashi S. Reduced beta-cell mass and expression of oxidative stress-related DNA damage in the islet of Japanese type II diabetic patients. *Diabetologia* 2002;45:85–96
53. Anvari E, Wikström P, Walum E, Welsh N. The novel NADPH oxidase 4 inhibitor GLX351322 counteracts glucose intolerance in high-fat diet-treated C57BL/6 mice. *Free Radic Res* 2015;49:1308–1318